Pure & Appl. Chem., Vol. 63, No. 10, pp. 1495–1502, 1991.
Printed in Great Britain.

Fluids in pores: experimental and computer simulation studies of multilayer adsorption, pore condensation and critical-point shifts

Arie de Keizer*, Thomas Michalski and Gerhard H. Findenegg

Institute of Physical Chemistry, Ruhr University Bochum,
Postfach 102148, D4630 Bochum 1, FRG

Abstract - The phase behaviour of a fluid in mesopores just below the critical temperature (T_c) has been studied experimentally and by molecular dynamics simulations. Experimental results were obtained for the adsorption of sulfur hexafluoride (SF_6) on Controlled-Pore Glass (CPG-10) for reduced temperatures $T_r = T/T_c$ of 0.857, 0.920 and 0.985. Pore condensation occurs at the two lowest temperatures, whereas at the highest temperature ($T_r = 0.985$) a phase transition cannot be detected, indicating that the fluid inside the pore is in a supercritical state. It follows that the pore critical temperature (T_{cp}) is lower than the bulk critical temperature. An analysis of unstable and metastable limits for the underlying system is given. Molecular dynamics computer simulations have been performed for a system of Lennard-Jones molecules, where the parameters values chosen simulated the SF_6-CPG system. Phase transitions are only present for the lowest temperatures, but the isotherm at $T_r = 0.985$ increases monotonically in agreement with experiment. If the fluid-fluid interaction ε_{FF} is decreased, pore condensation occurs at higher relative fugacities f/f_{sat}. Pore condensation occurs closer to the saturation pressure as the radius R is increased, in agreement with the experimental findings.

1. INTRODUCTION

Considerable attention has been directed to the behaviour of fluids in narrow pores [1-8]. For mesopores (2-50 nm), adsorption is usually characterized by pore condensation and the occurrence of hysteresis. Two different kinds of mechanisms have been proposed in the literature. For an idealized infinite cylindrical pore, hysteresis is believed to be an intrinsic property of the phase transition, i.e. a metastable state is present. In many cases porous materials consist of pores of very irregular shapes and many interconnections. Due to the presence of narrow necks and connections between the pores, pore filling and emptying will take place at different pressures (network model). Our treatment is based on the former model.

In mesopores a multilayer film is adsorbed at the pore wall as the saturation pressure of the gas is approached. For large radii adsorption can be described either by a model for localized adsorption or by a model for non-localized adsorption on a planar surface [9]. In the Frenkel-Halsey-Hill (FHH) model the pore wall is covered by an adsorbed film of uniform thickness l due to a substrate potential extending beyond the first layer. The stability of the film depends not only on the long-range van der Waals interactions between the substrate and the film, but also on the surface tension and curvature of the liquid-vapour interface, R - l = a (where R is the radius of the pore). From the (quantum) hydrodynamic excitation spectrum and also from thermodynamic considerations it can be derived that the curved film becomes unstable at some critical thickness l_c, and the pore becomes completely filled at the pressure corresponding to this film thickness l_c. During the growth of the multilayer adsorbed film, there is a region of metastability at $l_m < l < l_c$ in which the unsymmetrical state of a film of thickness l_m in equilibrium with a partially filled pore is energetically more favourable than the symmetrical state of a thicker film ($l > l_m$). Accordingly, emptying of the completely filled pore occurs at a lower pressure (corresponding to the film thickness l_m) than pore filling.

The shape and extent of hysteresis loops depend on temperature. As the surface tension decreases with increasing temperature, the contribution of the surface energy decreases while the van der Waals contribution is effectively independent of temperature. Accordingly, the symmetrical state of a thick adsorbed film will remain stable up to increasingly greater film thicknesses l_c. It follows that pore condensation occurs closer to the saturation point and hysteresis loops shrink with increasing temperature. An interesting situation arises as the critical temperature of the fluid is approached. Modern theories for the criticality of fluids between plates (slit pores) [3] and in cylindrical pores [4, 5] predict the disappearance of a phase transition (and hysteresis) for fluids in narrow pores at temperatures below the critical temperature (T_c) of the bulk fluid, i.e. there exists a pore critical temperature (T_{cp}) significantly lower than T_c. This prediction is supported by recent computer simulation studies [6, 7] and can be rationalized by the argument that a fluid in a narrow cylindrical pore is intermediate between a three-dimensional fluid and a one-dimensional fluid for which no critical point exists at $T > 0$.

* Permanent address: Department of Physical and Colloid Chemistry, Wageningen Agricultural University, Dreijenplein 6, 6703 HB Wageningen, The Netherlands

The results of an experimental sorption study of a fluid in a mesoporous glass substrate presented in this paper, support the the predicted shift of the critical temperature in pores. In addition, results of a molecular dynamics computer simulation study for a fluid of spherical molecules in a cylindrical pore with a radius of about 16 molecular diameters are presented for a similar reduced fluid temperature range ($0.85 < T/T_c < 0.985$). In the first part of the paper we address the question of the stability of multilayer adsorbed films in pores at temperatures well below T_{cp} and some aspects of critical-point shifts.

2. THEORETICAL BACKGROUND

2.1 Multilayer adsorption, pore condensation and hysteresis

Saam and Cole [1] have advanced a theory on the dynamics and thermodynamics of liquid films in porous media, giving explicit expressions for the radius of dynamic instability, a_c, at which the symmetric cylindrical fluid film becomes unstable, and the metastable radius, a_m. Between a_c and a_m the unsymmetrical state with a partially filled pore becomes energetically favourable. The thermodynamics is shortly summarized below. Limiting equations are derived and the effect of temperature will be worked out.

As a model we assume an ideal infinite cylindrical pore with radius R (Fig. 1). The mutual interaction between adsorbate molecules and between the adsorbate and the atoms (interaction centers) of the wall is represented by a 12-6 Lennard-Jones potential:

$$u_{ij} = 4\varepsilon\left[(\sigma / r_{ij})^{12} - (\sigma / r_{ij})^{6}\right] \tag{1}$$

ε and σ being the characteristic energy and distance parameters for fluid-fluid and fluid-wall interactions, respectively. The multilayer adsorption is not only dependent on the fluid-wall and the fluid-fluid interactions but also on the surface tension γ of the liquid-vapour interface. The pressure difference across the interface is given by the Laplace equation:

$$P^l - P^g = -\frac{\gamma}{a} \tag{2}$$

where P^l and P^g are the liquid and vapour pressure at the interface and a is the radius of the liquid-vapour boundary. Assuming ideality of the vapour phase, the chemical potentials at the vapour and the liquid side of the interface are given by Eqns. 3 and 4.

$$\mu^g = \mu_o(P_{sat},T) + kT\ln\left(\frac{P^g}{P_{sat}}\right) + U(a) \tag{3}$$

$$\mu^l = \mu_o(P_{sat},T) - \frac{\gamma}{a\Delta\rho} + U(a) \tag{4}$$

Here P_{sat} is the saturated vapour pressure, $\Delta\rho = \rho_o^l - \rho_o^g$ is the difference in the orthobaric densities of liquid and vapour, and the adsorption potential U(a) is a perturbation energy [9], i.e. the difference in interaction energy of a fluid molecule at some point a = R - I with the wall, and a situation in which the wall material is replaced by the liquid material. At equilibrium, these chemical potentials must be equal to the chemical potential of the bulk vapour formally given by Eqn. 3 when we set U(a) = 0 and $P^g = P^g(\infty)$. In this way we obtain the adsorption isotherm

$$kT\ln\frac{P^g(\infty)}{P_{sat}} = U(a) - \frac{\gamma}{a\Delta\rho} \tag{5}$$

For a cylindrical interface, U(a) can be derived by integrating the Lennard-Jones interactions:

$$U(a) = \int_R^\infty dr'r' \int_0^{2\pi} d\theta' \int_{-\infty}^{+\infty} dz'\, u(a,r',\theta',z') \tag{6}$$

The exact solution of the integral can be given in terms of a hypergeometric function F. Usually, for multilayer adsorption and the description of the instability of the liquid film only the attractive part of the Lennard-Jones interaction is taken into account.

$$U^{att}(a) = U(a) = -\left(\frac{3\pi\alpha}{2R^3}\right) F\left(\frac{3}{2}, \frac{5}{2}; 1; \left(\frac{a}{R}\right)^2\right) \tag{7}$$

The gas-substrate van der Waals coefficient is given by $\alpha = (\pi/6)(n^S c_{SF} - n^F c_{FF}) = (2\pi/3)(n^S \varepsilon_{SF}\sigma^6 - n^F \varepsilon_{FF}\sigma^6)$, where n^S and n^F represent the number density of the substrate and liquid, respectively, c_{SF} and c_{FF} are the constants of the c/r^{m+3} pair

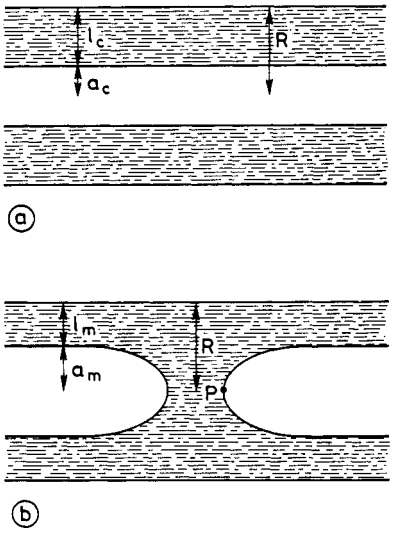

Fig.1. Schematic drawing of liquid in a cylindrical pore of radius R :
a. Multilayer adsorbed film at the instable limit a_c.
b. Unsymmetrical state of a partially filled pore at the metastable limit a_m.

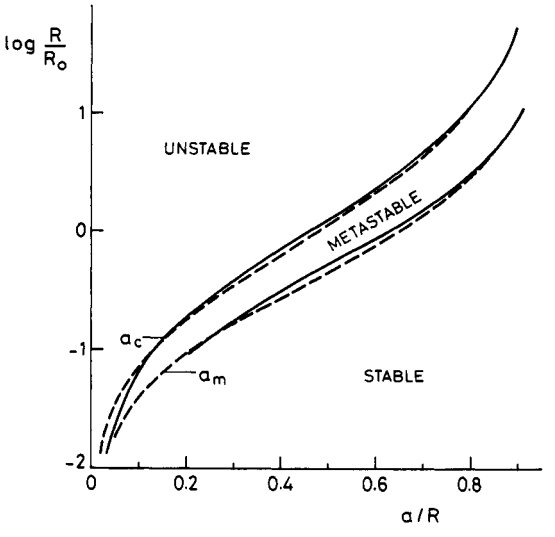

Fig. 2. Dependence of the unstable limit a_c/R.and the metastable limit a_m/R on the dimensionless variable R/R_o according to Eqns. 10 and 13 (full curves) and Eqns. 11 and 14 (dashed curves) respectively.

energies, while ε_{SF} ,σ_{SF} and ε_{FF} and σ_{FF} are the Lennard-Jones parameters for gas-substrate and gas-gas interactions (Eqn. 1). In the limit of large a (planar wall), this expression for U(a) reduces to

$$U(a) = -\frac{\alpha}{(R-a)^m} \tag{8}$$

with m = 3 in the case of non-retarded van der Waals interactions. In general, retardation effects should be taken into account, leading to deviations from Eqns. 7 and 8. However, Cheng and Cole [10] have shown that for cylindrical pores up to a diameter of 70 Å these are of minor importance and they are neglected in what follows.

Introduction of (7) or (8) into (5) leads to a modified FHH equation for multilayer adsorption in cylindrical pores. At small film thicknesses l = R–a, the adsorption potential U(a) will dominate the Laplace term, because the interaction of the film with the wall is strong and the curvature of the interface (1/a) is small. However, with increasing thickness the fluid-wall interactions become smaller whereas the curvature of the interface increases and thus the Laplace term becomes more negative. At some thickness l_c the cylindrical film becomes instable according to the stability criterion:

$$\frac{\partial \mu}{\partial l} = 0 \tag{9}$$

i.e. the adsorption isotherm becomes infinitely steep and at the given pressure the pore fills completely (pore condensation). From (5), (7) and (9) an equation for the critical thickness can be derived

$$\left(\frac{R}{R_o}\right)^2 = \frac{y_c^2}{\left(1-y_c^2\right)^{5/2}} P^1_{3/2}\left[\frac{\left(1+y_c^2\right)}{\left(1-y_c^2\right)}\right] \tag{10}$$

Here $R_o = (3\pi\alpha\Delta\rho/\gamma)^{0.5}$ is a scaling parameter dependent on the properties of the chosen materials, and $y_c = a_c/R$. $P^1_{3/2}$ is an associated Legendre function. In the limit of large a it follows from Eqns. 5, 8 and 9 that

$$\frac{R}{R_o} = \frac{1}{\sqrt{\pi}} \frac{y_c}{\left(1-y_c\right)^2} \tag{11}$$

Graphs of R/R_o against y_c according to Eqns. 10 and 11 are presented in Fig. 2.

During the growth of the multilayer adsorbed film to a thickness a_c we have entered a metastable region in which the free energy would be lowered if the fluid could reach the unsymmetrical state of a partly filled pore in equilibrium with a cylindrical film of thickness a_m. During desorption this unsymmetrical state occurs (Fig. 1b). The equilibrium situation between surfaces

with different curvatures is now given by

$$kT\ln\frac{P^g(\infty)}{P_{sat}} = U(r) - \frac{\gamma}{\Delta\rho}\left(\frac{1}{r_1}+\frac{1}{r_2}\right) \tag{12}$$

where r is the radial position of a point on the surface, and r_1 and r_2 are the two curvature radii for this point. At $r = a_m$ we have $(1/r_1 + 1/r_2)=1/a_m$, whereas at $r = 0$, $r_1 = r_2 \neq a_m/2$. As U varies between $r = 0$ and $r = a_m$ it is clear that the curvature of the meniscus is not constant but also a function of r; specifically, the meniscus is not spherical in the center of the pore.

The thickness a_m can be derived by minimizing the free energy for the unsymmetrical state.

$$2a_m^{-2}\int_0^{a_m} dr\, r U(r) = U(a_m) + \frac{\gamma}{a_m\Delta\rho} \tag{13}$$

Introducing Eqn.7 into Eqn. 13 results in an explicit equation for R/R_o as a function of $y_m=a_m/R$.

$$\left(\frac{R}{R_o}\right)^2 = \frac{F\left(\frac{3}{2},\frac{5}{2};1;y_m^2\right)y_m}{2} - \frac{\int_0^{y_m} F\left(\frac{3}{2},\frac{5}{2};1;y^2\right)y\,dy}{y_m} \tag{13a}$$

The metastable limit a_m must be larger than the instability limit a_c. If the limiting equation (8) is introduced in Eqn.13 instead of Eqn.(7) the integral can be solved easily leading to Eqn.14.

$$\frac{R}{R_o} = \frac{1}{\sqrt{3\pi}}\frac{y_m}{(1-y_m)^{3/2}} \tag{14}$$

The dependence of a_m/R on R/R_o according to Eqns. 13a and 14 is also given in Fig. 2. It appears that the limiting equations give satisfactory results for a wide range of R/R_o. For large R, the limiting curves coincide with the exact curves according to Eqns. 10 and 13a.

2.2 Behaviour near the critical point

The Cole-Saam theory outlined above is based on a simple slab model of a liquid-like adsorbed film in equilibrium with the gas phase. The effect of temperature on the phase stability in the pore is contained in the scaling parameter R_o (see Eqns. 10, 11, 13a and 14). The van der Waals interaction parameter $\alpha = (2\pi/3)(n^S\varepsilon_{SF}\sigma^6 - n^F\varepsilon_{FF}\sigma^6)$ is expected to increase with temperature as the density of the liquid-like film (n^F) decreases. A more pronounced temperature dependence of R_o is caused by the surface tension γ and the density increment $\Delta\rho$ as the critical temperature of the fluid (T_c) is approached. Sufficiently close to criticality, γ and $\Delta\rho$ approach zero according to the asymptotic power laws

$$\gamma = \gamma_o t^{\mu}; \qquad \Delta\rho \equiv \rho_o^l - \rho_o^g = B_o t^{\beta} \tag{15}$$

Here, $t = (T_c-T)/T_c$ is the dimensionless distance from the critical temperature, μ and β are 3d-Ising-like critical exponents ($\mu = 1.26$, $\beta = 0.32$) and γ_o, B_o are non-universal critical amplitudes. Accordingly, R_o will increase with decreasing t and will tend to infinity for $t\to 0$ as $R_o \sim t^{-\phi}$ with $\phi = (\mu-\beta)/2 \approx 0.47$. From Fig. 2 it follows that for a given fluid/substrate system both the metastable and instable limits are shifted to lower values of a (larger film thickness) when temperature is increased. Accordingly, pore condensation will occur closer to the saturation pressure P_{sat} and the hysteresis loop shrinks when T approaches T_c. Such a behaviour was indeed found experimentally [4].

Novel results for the behaviour of fluids in pores have been obtained by recent studies in statistical mechanics. In a pioneering work by Fisher and Nakanishi [3] on the criticality of fluids between plates, it was shown that the critical behaviour is affected both by the finite thickness of the fluid film and by its interactions with the wall. In particular, this scaling theory predicts that pore condensation and the related hysteresis disappear at some temperature T_{cp} below the bulk critical temperature T_c. The critical temperature shift $\Delta T_c \equiv T_c - T_{cp}$ is dictated by the ratio of the pore width D and the correlation length ξ of the microscopic density fluctuations in the bulk fluid. In the absence of any fluid-wall interactions, the theory gives

$$\xi(\Delta T_c) \approx 0.346D \tag{16}$$

where $\xi(\Delta T)$ is the value of ξ at $\Delta T = T_c - T$. Near the critical point, the correlation length of the fluid varies as $\xi(t) = \xi_o t^{-\nu}$ with $\nu = 0.63$ and the factor ξ_o is of the order of magnitude of the molecular diameter σ_{FF}. Accordingly, one expects $\Delta T_c/T_c \approx 5.4(D/\xi_o)^{-1/\nu}$, e.g. $\Delta T_c \approx 20$ K for $D = 5$ nm, $\xi_o = 0.3$ nm and $T_c = 300$ K. Even larger critical point shifts are predicted for the case of a (short-ranged) attractive fluid-wall interaction [3]. The phenomenon of critical-point shifts in a slit-like geometry can be rationalized by the argument that the fluid is between a three-dimensional state ($D \to \infty$) and a two-dimensional state ($D \to \sigma$), and the fact that $T_c(2d)$ is much smaller than $T_c(3d)$ for a given pair potential [4].

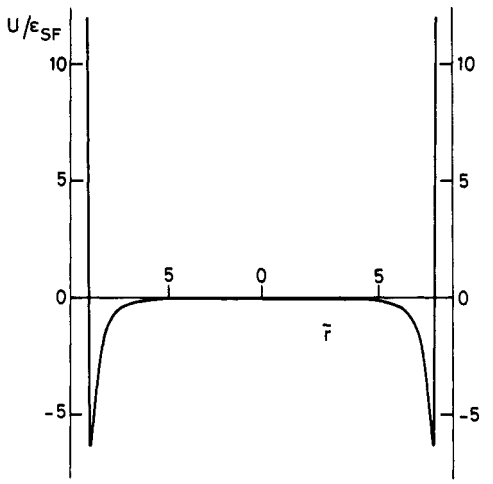

Fig.3. Fluid-wall potential U/ε_{SF} for a SF_6 molecule in a cylindrical CPG-pore ($\tilde{R}$=8.19, ε_{SF}/k=220.5 K and η=0.077 Å^{-2}).

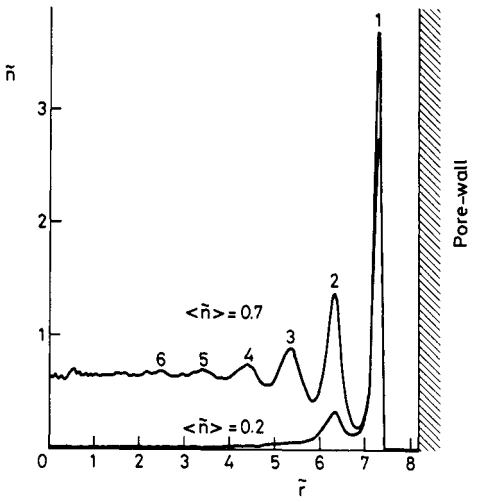

Fig.4. One-dimensional density profiles for the adsorption of SF_6 in a CPG-pore at two overall pore densities <ñ> ($\tilde{R}$=8.19, ε_{FF}/k=265.6 K and ε_{SF}/k=220.5 K).

The situation in a cylindrical pore was investigated on the basis of a mean-field lattice gas model by Nicholson [2] and more recently by means of a density functional approach by Evans et al. [4]. In both cases, phenomena closely related to critical-point shifts were found, although their true nature is somewhat obscure since in the limit $R \rightarrow \sigma/2$ the pore fluid becomes one-dimensional and would not undergo pore condensation.

3. MOLECULAR DYNAMICS COMPUTER SIMULATIONS

We are investigating the state of a fluid of spherical molecules in ideal cylindrical pores by means of Molecular Dynamics (MD) simulations. The aim of this work is to study the influence of pore width and the relative strengths of fluid-substrate and fluid-fluid interactions on the thickness of the adsorbed film, as well as the disappearance of pore condensation at near-critical temperatures. The parameters were chosen just to mimic the sorption of sulfur hexafluoride (SF_6) in a Controlled-Pore Glass (CPG-10) which we are studying experimentally over a range of reduced temperatures near the critical point of SF_6 (see next section).

The MD simulations are performed on a CYBER 205 vector computer for a system of Lennard-Jones molecules. The program used was developed by Heinbuch and Fischer [7,12]. Newton's second-order differential equations of motion were solved by using a fifth-order predictor corrector algorithm due to Gear [13]. The LJ parameters of the fluid were estimated from saturated vapour pressure data for SF_6 according to Lustig [14].

In the MD simulations the particles are placed initially in a number of monolayers (depending on the overall density $\langle\tilde{n}\rangle = \langle n\rangle\sigma_{FF}^3$) perpendicular to the cylinder axis. This procedure does not enable us to simulate the adsorption and desorption branches separately. Periodic boundary conditions and a minimum image criterion are applied in the axial direction. The height of the central cylinder H was generally chosen as 9.097 σ_{FF} and <ñ> was between 0.05 and 0.7. The maximum number of particles in the central cylinder was 1180.

Calculations were performed with σ_{FF} = 4.7 Å and two ε_{FF}/k values (265.57 K and 245.0 K). The pore diameter was estimated to $\tilde{R} = R/\sigma_{FF}$ = 8.19. The solid adsorbent was modelled as a number of concentric cylindrical surfaces with a distance d = 3.60 Å and a surface density η as 0.077 Å^{-2} analogous to the model used earlier for graphite [14]. Although this model is less appropriate for an SiO_2 lattice, the detailed structure of the solid will not have great influence on our results. The LJ parameters for the fluid-wall interaction corresponding to the assumed values of η and d were estimated from the initial slope of the experimental adsorption isotherm. Values of σ_{SF} = 4.15 Å and ε_{SF} = 220.5 K were assumed. The potential $U_{SF}(r)$ of an SF_6 molecule at a distance r from the surface was obtained by integration of the interaction in 6 concentric shells. The function U_{SF} (r) was accurately approximated by two polynomials. The potential profile is displayed in Fig. 3. In this typical case of a relatively large pore radius, the potential is only effective near the wall.

Long-range corrections were calculated above a cut-off radius of 3.5 σ_{FF}. The long-range correction in the total internal energy amounted to 4% or less. The chemical potential of the pore fluid was obtained by the modified test particle method, by introducing a test particle at 500 randomly chosen positions after every 4 time steps set to 0.005 $\sigma(m/\varepsilon_{FF})^{1/2}$, where m is the molecular mass of SF_6. Generally, 10,000 equilibration time steps and 20,000 production time steps appeared to be

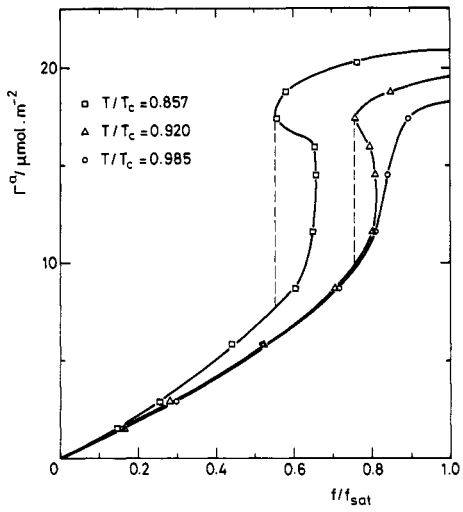

Fig.5 Sorption isotherms (adsorbed amount Γ^a vs. relative fugacity f/f_{sat}) at three temperatures calculated by MD simulations ($\tilde{R}$=8.19, ε_{FF}/k=265.6 K and ε_{SF}/k=220.5 K)

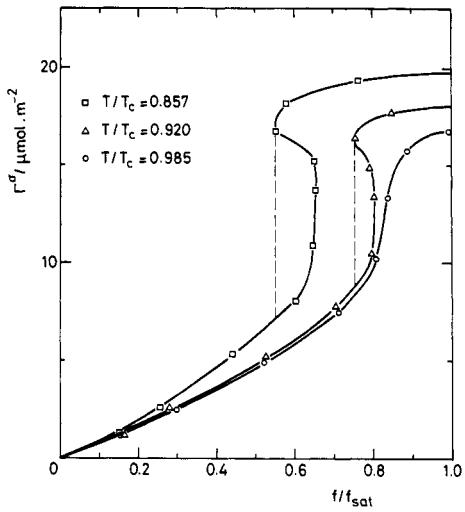

Fig.6 Sorption isotherms (surface excess Γ^σ vs. relative fugacity f/f_{sat}) at three temperatures calculated by MD simulations ($\tilde{R}$=8.19, ε_{FF}/k=265.6 K and ε_{SF}/k=220.5 K)

satisfactory in the present NVT ensemble. One-dimensional density profiles for two overall densities of the pore fluid are shown in Fig. 4. At $\langle\tilde{n}\rangle$=0.2, most molecules are in a layer next to the wall and in a second layer. At $\langle\tilde{n}\rangle$=0.7, pore condensation has taken place. Here the layering of the fluid induced by the wall persists to ca. 6 layers and the fluid density in the center of the pore is almost equal to the mean density $\langle\tilde{n}\rangle$.

Isotherms of the total number of particles in the pore (per unit area of the pore wall) are plotted as a function of the relative fugacity $f/f_{sat}=\exp(\mu/kT-\mu_{sat}/kT)$ in Fig.5. The chemical potential μ was obtained by the test particle method as explained above. The value of μ_{sat} was obtained from the Haar-Shenker-Kohler equation [19]. Experimentally, one measures the surface excess concentration Γ^σ rather than the absolute concentration Γ^a. For given pore radius R and gas density ρ^g, these two concentrations are related by

$$\Gamma^a = \Gamma^\sigma + \rho^g R/2 \qquad (17)$$

It follows that Γ^σ is lower than Γ^a, particularly at higher pressures (Fig.6). At high gas densities the adsorption isotherm Γ^σ vs. f/f_{sat} can even go through a maximum as has been found in some experimental cases (see below).

S-shape isotherms are found at reduced temperatures T_r = 0.857 and 0.920, but the isotherm at T_r = 0.985 increases monotonically in agreement with experiment. The S-shape gives the extent of the hysteresis loop, which is larger for the lowest temperature. If the fluid - fluid interaction is decreased, pore condensation occurs at higher relative fugacities f/f_{sat}(Fig.7), where the extent of the hysteresis loop occurring at T_r = 0.857 is decreased. Although calculations have not been performed at T_r = 0.920 for this lower ε_{FF}/k, it is expected from the width of the hysteresis loops that the pore-critical temperature increases with increasing ε_{FF}. If we compare our results at large pore radius with Heinbuch's results for argon at smaller radius [7], condensation may be expected to occur closer to the saturation pressure and the pore critical temperature increases, if R/σ is increased. The relative positions of the isotherms at different temperatures are in agreement with the experimental results, i.e. adsorption decreases with increasing temperature indicating that the adsorption is more exothermic than condensation of the bulk fluid.

Systematic investigations of the separate adsorption and desorption branches at different ε_{FF}, ε_{SF} and R/σ_{FF} are still in progress [16].

4. EXPERIMENTAL RESULTS AND DISCUSSION

Adsorption-desorption isotherms of SF_6 (T_c=318.7 K) on CPG-10 were obtained by gravimetric measurements in a pressure range from ca 1.5 bar up to nearly the critical pressure (p_c=37.6 bar) using a Sartorius high pressure microbalance. CPG-10 is prepared by Electro-Nucleonics Inc. (New Jersey, USA) and is available with mean pore diameters ranging from 7.5 nm to 500 nm. Except for the low end of the pore size range, typically more than 80% of the pores in CPG-10 have pore diameters within ± 10% of the nominal diameter. In the present work, results for CPG-10 with mean pore diameter 7.7 nm are presented. Experimental details and results for other pore sizes will be published elsewhere [17].

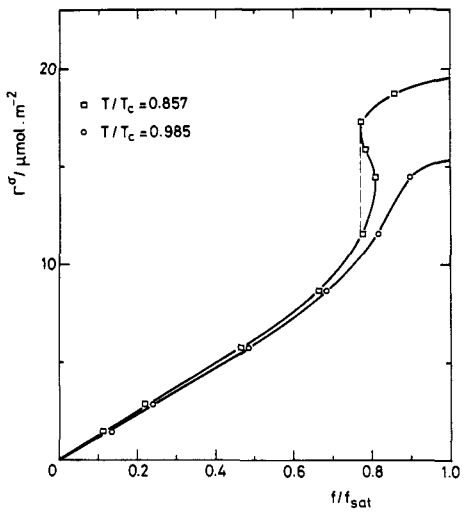

Fig.7. Sorption isotherms (surface excess Γ^{σ} vs. relative fugacity f/f_{sat}) at two temperatures calculated by molecular dynamics simulations ($\tilde{R}$=8.19, ε_{FF}/k=245.0 K and ε_{SF}/k=220.5 K).

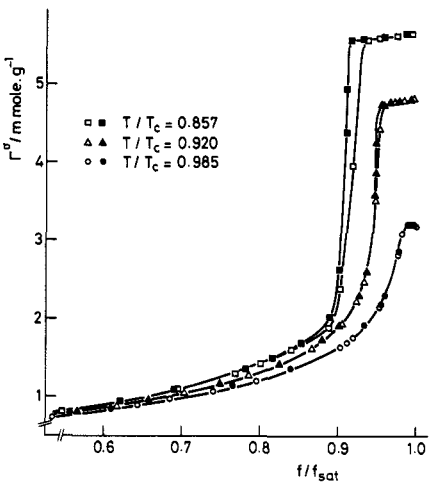

Fig.8. Sorption isotherms (surface excess Γ^{σ} vs. relative fugacity f/f_{sat}) for SF_6 on Controlled - Pore Glass (CPG-10) at three temperatures (□, △, ○ adsorption experiment; ■, ▲, ● desorption experiment)

Surface excess amounts for SF_6 in CPG-10 (7.7 nm) at three T_r values (0.857, 0.920 and 0.985) in the fugacity range f/f_{sat} from 0.5 to 1.0 are shown in Fig. 8. According to the manufacturer, the specific surface area of the present CPG-10 sample is 182 m^2/g, the pore volume is 0.47 ml/g and more than 80% of the pore volume is in the pore diameter range from 7.2 to 8.2 nm. The affinity of SF_6 for this substrate is relatively low and the adsorption increases almost linearly with the fugacity below f/f_{sat}=0.5 (not shown in Fig. 8). The weak temperature dependence of the adsorption as a function of f/f_{sat} indicates that the differential molar enthalpy of adsorption is a little larger than the enthalpy of condensation. At T_r=0.857, condensation commences at f/f_{sat}=0.89 and this isotherm exhibits a pronounced hysteresis loop. A much smaller loop with a lower closure point at f/f_{sat}=0.95 is exhibited by the isotherm at T_r=0.920. At T_r=0.985 no loop can be detected, indicating the absence of condensation. The pore fluid is then in a supercritical state and appears to have a lower critical temperature than the bulk fluid.

The present results are consistent with those of a related work by Nuttall and Everett [18], who studied the sorption of xenon in Vycor glass, which has somewhat smaller pores and (presumably) a wider distribution of pore sizes than the controlled-pore glass used here. Accordingly, their ascending and descending branches are less steep, but its gradual shrinking and eventual disappearance as temperature increases towards T_c was apparant as in our experiments. This behaviour is consistent with our MD computer simulation results, where at the highest temperature hysteresis was also absent.

It is noticed experimentally that condensation occurs at relatively high f/f_{sat} and that loops are narrow. This is probably connected with the high pore radius of CPG. A second remark can be made with respect to the plateau values (pore-filling) of the sorption isotherms at different temperatures. The large difference in plateau values can be explained by differences in $\Delta\rho$ at different temperatures as will be shown below. The maximum at the highest temperature is due to the effect of the bulk density on the surface excess, as has also been shown for our MD results.

The surface excess amounts are expressed in μmol/g. After calculation of the adsorption in μmol/m^2 with the specific surface area given, we can estimate the thickness of the adsorbed layer l_s with the slab model corrected for the compression of the liquid boundary layer [11].

$$\Gamma^{\sigma} = \left(\rho_o^l - \rho_o^g\right) \cdot l_s \left(1 - \frac{l_s}{2R}\right) + \left(\rho_m - \rho_o^l\right)\xi \qquad (18)$$

Here ρ_o^l, ρ_o^g and ρ_m (=12.66 kmol/m^2) are the orthobaric densities of the liquid, the vapour at the given temperature and the triple point density of the bulk liquid respectively. The parameter ξ (=0.523 nm) is a (temperature-independent) decay length [11]. The thickness obtained from the plateau value must be equal to the pore radius as complete pore filling has occurred. The radius obtained in this way appears to be fully independent of temperature, i.e. the differences in plateau values are perfectly explained by $\Delta\rho$ values at the different temperatures. However, the pore diameter amounts to 120.8 ± 0.8 Å, in disagreement with the manufacturer's value. The diameter obtained from the pore volume and the specific surface area, 103 Å, also deviates appreciably. At present it is a matter of discussion whether the diameter is erroneous or if the specific surface area has been determined incorrectly.

According to Eqns. 7 and 8, the fluid-wall interaction can be expressed in terms of the characteristic interaction coefficient α. In principle α can be determined by fitting the experimental isotherms in the multilayer region to the modified FFH equation. Although the fit was rather poor, a rough estimate for α (at T/T_c=0.857) gave a value within the range of 1.2-1.5 eV Å^3. It follows that R_o = 1.6 nm and log R/R_o = 0.57. From Fig.2, the values of a_c/R and a_m/R can be estimated to 0.66 and 0.81 respectively. From the adsorption isotherm, it can be derived that condensation would start at 3.2 mmol/g, whereas the desorption branch of the hysteresis loop ends at 2.1 mmol/g. The latter value corresponds perfectly with the value obtained from the experimental desorption isotherm (Fig. 8). However, it seems that in the experimental adsorption isotherm, condensation starts below 3.2 mmol/g. This may be attributed to fluctuation in the lining of the pore wall which then varies the effective pore diameter. It is found that the width of the hysteresis loop is overestimated by the Saam and Cool theory as well as by MD simulations. This may also be due to simplications of the pore geometry in our model.

CONCLUSIONS

The state of a fluid in pores at temperatures somewhat below the bulk critical temperature T_c has been studied experimentally by adsorption measurements and by MD computer simulations. Adsorption isotherms of SF_6 in CPG change phenomenologically from subcritical behaviour (with the appearance of pore condensation and hysteresis) to a supercritical behaviour without these features. For the present substrate (mean pore diameter 7.7 nm), the isotherm at T/T_c=0.92 is marginally below the pore critical temperature (T_{cp}). Qualitatively, these features are also found in the MD study of the Lennard-Jones fluid in an infinite cylindrical pore. The noticable difference in the width of the hysteresis loop and other differences in the two sets of results may be due to the oversimplified pore model underlying the simulations. Nonetheless, the qualitative similarity of these results supports the conjecture that the disappearance of hysteresis at temperatures $T < T_c$ is an intrinsic feature of fluids in pores (and is not caused by percolation in a network). The MD simulations reveal that a decreasing strength of the fluid-fluid pair interaction (at given strength of the fluid-wall interaction) causes a pronounced shift of pore condensation toward higher relative pressures. Further work to clarify the influence of the strength of fluid-fluid and fluid-wall interactions and of the pore diameter on the critical-point shift T_c-T_{cp} is now in progress.

Acknowledgements

Thanks are due to Prof. J. Fischer and Dr. S. Sokolowski for useful suggestions concerning the MD calculations.

REFERENCES

1. M.W. Cole and W.F. Saam, *Phys. Rev. Lett. 32*, 985-988 (1974).
   W.F. Saam and M.W. Cole, *Phys. Rev. B. 11*, 1086-1105 (1975).
2. D. Nicholson, *J. Chem. Soc. Faraday Trans. 1, 71*, 238-255 (1975).
3. M.E. Fisher and H. Nakanishi, *J. Chem. Phys. 75*, 5857-5863 (1981); H. Nakanishi and M.E. Fisher, *ibid 78*, 3279-3293 (1983).
4. R. Evans, U. Marini Bettolo Marconi and P. Tarazona, *J. Chem. Phys. 84*, 2376-2398 (1986); *J. Chem. Soc., Faraday Trans. 2, 82*, 1763-1787 (1986); P. Tarazona, U. Marini Bettolo Marconi and R. Evans, *Mol. Phys. 60*, 573-595 (1987).
5. E. Bruno, U. Marini Bettolo Marconi and R. Evans, *Physica 141A*, 187-210 (1987).
6. A.Z. Panagiotopoulos, *Mol. Phys. 61*, 813-826 (1987); *62*, 701-719 (1987).
7. U. Heinbuch and J. Fischer, *Chem. Phys. Letters 135*, 587-590 (1987).
   U. Heinbuch, *VDI - Fortschrittsberichte*, Reihe 3 nr. 173, VDI Verlag, Düsseldorf (1989).
8. B.K. Peterson, K.E. Gubbins, G.S. Heffelfinger, U. Marini Bettolo Marconi and F. van Swol, *J.Chem.Phys. 88*, 6487-6500 (1988).
9. W.A. Steele, *The Interaction of Gases with Solid Surfaces*, Pergamon Press, Oxford (1974) Chap. 5.
10. E. Cheng and M.W. Cole, *Langmuir 5*, 616-625 (1989).
11. Th. Michalski, A. Benini and G.H. Findenegg, *Langmuir*, accepted (1990).
12. U. Heinbuch and J. Fischer, *Molecular Simulation 1*, 109-120 (1987).
13. C.W. Gear, Numerical initial value problems in ordinary differential equations, Prentice Hall, Englewood Cliffs (1971).
14. R. Lustig, *Fluid Phase Equilibria 32*, 117-137 (1987).
15. J. Fischer, M. Bohn, B. Körner and G.H. Findenegg, *German Chem. Eng. 6*, 84-91 (1983).
16. A. de Keizer, J. Fischer and G.H. Findenegg, to be published.
17. Th. Michalski and G.H. Findenegg, to be published.
18. C.G.V.Burgess, D.H.Everett and S.Nuttall, *Pure Applied Chem. 61*, 1845-1852 (1989).
    Also reported in : P.C. Ball and R. Evans, *Langmuir 5*, 714-723 (1989).
19. J. Fischer and M. Bohn, *Mol.Phys. 58*, 395-399 (1986).